ADIABATIC QUANTUM PUMPING IN BUCKLED GRAPHENE NANORIBBON DRIVEN BY A KINK*

DOMINIK SUSZALSKI, ADAM RYCERZ

Institute of Theoretical Physics, Jagiellonian University
Łojasiewicza 11, 30-348 Kraków, Poland

We propose a new type of quantum pump in buckled graphene nanoribbon, adiabatically driven by a kink moving along the ribbon. From a practical point of view, pumps with moving scatterers present advantages as compared to gate-driven pumps, like enhanced charge transfer per cycle per channel. The kink geometry is simplified by truncating the spatial arrangement of carbon atoms with the classical ϕ^4 model solution, including a width renormalization following from the Su–Schrieffer–Heeger model for carbon nanostructures. We demonstrate numerically, as a proof of concept, that for moderate deformations, a stationary kink at the ribbon center may block the current driven by the external voltage bias. In the absence of a bias, a moving kink leads to a highly-effective pump effect, with a charge per unit cycle dependent on the gate voltage.

1. Introduction

The idea of quantum pumping, *i.e.*, transferring the charge between electronic reservoirs by periodic modulation of the device connecting these reservoirs [1], has been widely discussed in the context of graphene nanostructures [2–8]. Since early works, elaborating the gate-driven pumping mechanism in graphene [2] and bilayer graphene [3], it becomes clear that the transport via evanescent modes may significantly enhance the effectiveness of graphene-based pumps compared to other quantum pumps. Other pumping mechanisms considered involve laser irradiation [4], strain fields [5], tunable magnetic barriers [6], Landau quantization [7], or even sliding the Moiré pattern in twisted bilayer graphene [8].

It is known that quantum pump with a shifting scatterer may show enhanced charge transfer per cycle in comparison to a standard gate-driven

---

* Presented at the 45$^{\text{th}}$ Congress of Polish Physicists, Kraków, September 13–18, 2019.

pump [1], see also Fig. 1 (a)[1]. Motivated by this conjecture, we consider a buckled nanoribbon, see Fig. 1 (b), similar to the one studied numerically by Yamaletdinov *et al.* [9, 10] as a physical realization of the classical ϕ^4 model and its topological solutions (*kinks*) connecting two distinct ground states. Our setup is supplemented with two heavily-doped graphene leads, attached to the clamped edges of a ribbon, allowing to pass electric current along the system.
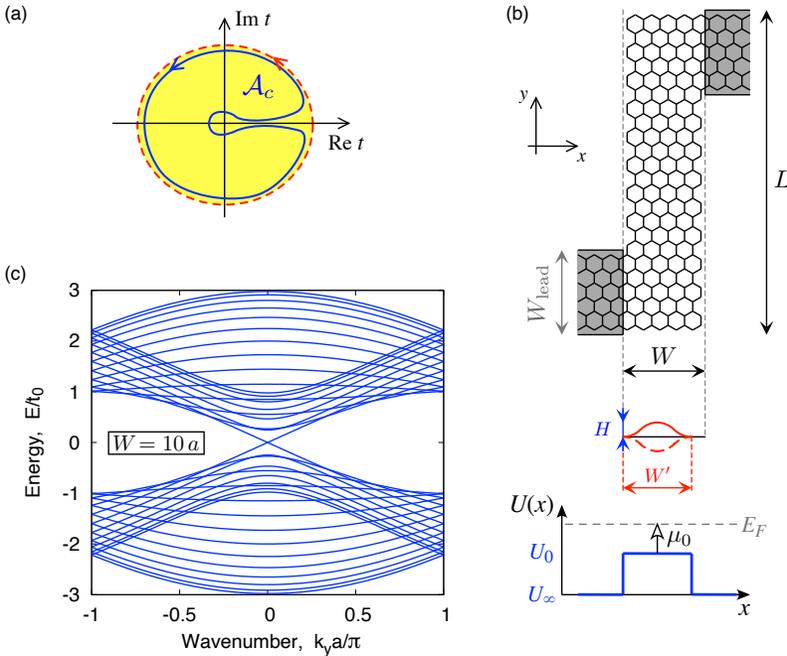

Fig. 1. (Color online) Buckled graphene nanoribbon as a quantum pump. (a) Typical pumping cycles (schematic) for a single channel characterized by the complex transmission amplitude, $t = \operatorname{Re} t + i \operatorname{Im} t$. Blue solid line enclosing the area $\mathcal{A}_c$ shows one-parameter cycle allowed for a standard gate-driven pump, red dashed line corresponds to the cycle involving a shift of a scatterer. (b) Flat ribbon with armchair edges attached to heavily-doped graphene leads (shaded areas). The ribbon width $W = 5\,a$ (with $a = 0.246\,\text{nm}$ the lattice spacing) and length $L = 11.5\sqrt{3}\,a$ are chosen for illustrative purposes only. A cross section of buckled ribbon, characterized by the reduced width $W' < W$ and the buckle height $H > 0$, and the electrostatic potential energy profile $U(x)$, are also shown. (c) Band structure of the infinite metallic-armchair nanoribbon of $W = 10\,a$ width, the same as used in the computations.

---

[1] In the simplest case of a one-parameter driven, one-channel pump, the charge per cycle is given by $Q = (e/\pi)\mathcal{A}_c$, with $\mathcal{A}_c$ being the $\pm$ area enclosed by the contour in the $(\operatorname{Re} t, \operatorname{Im} t)$ plane (where t is a parameter-dependent transmission amplitude).

2. Model and methods

The analysis starts from the Su–Schrieffer–Heeger (SSH) model for the ribbon, including the hopping-matrix elements corresponding to the nearest-neighbor bonds on a honeycomb lattice [11–14]

$$\mathcal{H}_{\text{ribbon}} = -t_0 \sum_{\langle ij\rangle,s} \exp\left(-\beta\frac{\delta d_{ij}}{d_0}\right)\left(c_{i,s}^\dagger c_{j,s} + c_{j,s}^\dagger c_{i,s}\right) + \frac{1}{2}K\sum_{\langle ij\rangle}(\delta d_{ij})^2 \ , \quad (1)$$

with a constrain $\sum_{\langle ij\rangle}\delta d_{ij} = 0$, where δd_{ij} is the change in bond length, and $d_0 = a/\sqrt{3}$ is the equilibrium bond length defined via the lattice spacing $a = 0.246\,\text{nm}$. The equilibrium hopping integral $t_0 = 2.7\,\text{eV}$, $\beta = 3$ is the dimensionless electron–phonon coupling, and $K \approx 5000\,\text{eV}/\text{nm}^2$ is the spring constant for a C–C bond. The operator $c_{i,s}^\dagger$ (or $c_{i,s}$) creates (or annihilates) a π electron at the ith lattice site with spin s.

In order to determine the spatial arrangement of carbon atoms in a buckled nanoribbon, $\{\boldsymbol{R}_j = (x_j, y_j, z_j)\}$, we first took the $\{x_j\}$ and $\{y_j\}$ coordinates the same as for a flat honeycomb lattice in the equilibrium and set $\{z_j\}$ according to

$$z = H\tanh\left(\frac{y - y_0}{\lambda}\right)\sin^2\left(\frac{\pi x}{W}\right) \ , \quad (2)$$

representing a topologically non-trivial solution of the ϕ^4 model, with H the buckle height, W the ribbon width, y_0 and λ the kink position and size (respectively). Next, x-coordinates are rescaled according to $x_j \to x_j W'/W$, with W' adjusted to satisfy $\sum_{\langle ij\rangle}\delta d_{ij} = 0$ in the $y_0 \to \pm\infty$ (*no kink*) limit. In particular, $H = 2\,a$ and $W = 10\,a$ corresponds to $W'/W = 0.893$. We further fixed the kink size at $\lambda = 3\,a$ (closely resembling the kink profile obtained from the molecular dynamics in Ref. [9]); this results in relative bond distorsions not exceeding $|\delta d_{ij}|/d_0 \leqslant 0.08$. Full optimization of the bond lengths in the SSH Hamiltonian (1), which may lead to the alternating bond pattern [14], is to be discussed elsewhere.

Heavily-doped graphene leads, $x < 0$ or $x > W'$ in Fig. 1 (b), are modeled as flat regions ($d_{ij} = d_0$) with the electrostatic potential energy $U_\infty = -0.5t_0$ (compared to $U_0 = 0$ in the ribbon), corresponding to 13 propagating modes for $W_\infty = 20\sqrt{3}\,a$ and the chemical potential $\mu_0 = E_{\text{F}} - U_0 = 0$. The scattering problem is solved numerically, for each value of the chemical potential μ_0 and the kink position y_0, using the Kwant package [15] allowing to determine the scattering matrix

$$S(\mu_0, y_0) = \begin{pmatrix} r & t' \\ t & r' \end{pmatrix} \ , \quad (3)$$

which contains the transmission t (t') and reflection r (r') amplitudes for charge carriers incident from the left (right) lead, respectively.

The linear-response conductance can be determined from the S-matrix via the Landuer–Büttiker formula [1], namely

$$G = G_0 \mathrm{Tr}\, tt^\dagger = \frac{2e^2}{h} \sum_n T_n \,, \tag{4}$$

where $G_0 = 2e^2/h$ is the conductance quantum and T_n is the transmission probability for the nth normal mode. Similarly, in the absence of a voltage bias, the charge transferred between the leads upon varying solely the parameter y_0 is given by

$$\Delta Q = -\frac{ie}{2\pi} \sum_j \int \mathrm{d}y_0 \left(\frac{\partial S}{\partial y_0} S^\dagger \right)_{jj} \,, \tag{5}$$

where the summation runs over the modes in a selected lead. Additionaly, the integration in Eq. (5) is performed for a truncated range of $-\varLambda \leqslant y_0 \leqslant L + \varLambda$, with $\varLambda = 250\, a \gg \lambda$ for $L = 75.5\sqrt{3}\, a$.

3. Results and discussion

In Fig. 1 (c), we depict the band structure for an infinite (and flat) metallic-armchair ribbon of $W = 10\, a$ width. It is remarkable that the second and third lowest-lying subband above the charge-neutrality point (as well as the corresponding highest subbands below this point) show an almost perfect degeneracy near their minima corresponding to $E_{\mathrm{min}}^{(2,3)} \approx 0.25\, t_0$, which can be attributed to the presence of two valleys in graphene. For higher subbands, the degeneracy splitting due to the trigonal warping is better pronounced.

The approximate subband degeneracy has a consequence for the conductance spectra of a finite ribbon, presented in Fig. 2: For both the flat ribbon ($H = 0$) and a buckled ribbon with no kink ($H = 2\, a$, $y_0 \to -\infty$), the conductance $G \approx G_0$ for $|\mu_0| < E_{\mathrm{min}}^{(2,3)}$ and quickly rises to $G/G_0 \approx 2.5$–3 for $\mu > E_{\mathrm{min}}^{(2,3)}$. For $\mu < 0$, the quantization is not so apparent, partly due the presence of two p–n interfaces (at $x = 0$ and $x = W'$) leading to stronger-pronounced oscillations (of the Fabry–Perrot type), and partly due to a limited number of propagating modes in the leads. For a kink positioned at the center of the ribbon ($H = 2\, a$, $y_0 = L/2$), the conductance is strongly suppressed, $G \ll G_0$, in the full $|\mu_0| < E_{\mathrm{min}}^{(2,3)}$ range (with the exception from two narrow resonances at $\mu_0 = \pm 0.1327\, t_0$, which vanishes for $y_0 \neq L/2$) defining a feasible energy window for the pump operation.
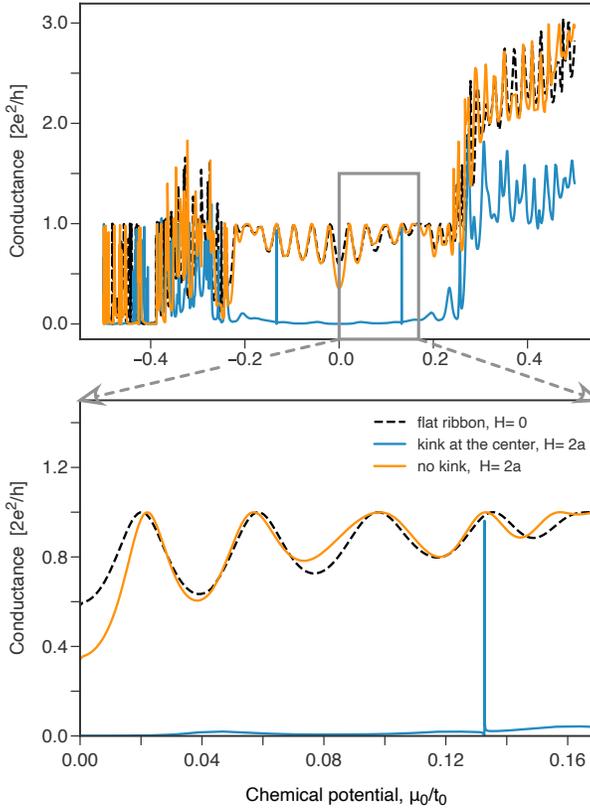
Fig. 2. (Color online) Conductance of the ribbon with $W = 10\,a$ as a fuction of the chemical potential. The remaining parameters are $L = 75.5\sqrt{3}\,a$ and $W_{\text{lead}} = 20\sqrt{3}\,a$. Different lines (the same in two panels) correspond to the flat ribbon geometry, $H = 0$, $W' = W$ (black dashed), the buckled ribbon with $H = 2\,a$ and $y_0 = L/2$ (black/blue solid) or $y_0 \to -\infty$ (gray/orange solid); see Eq. (2). Bottom panel is a zoom-in of the data shown in top panel.

In Fig. 3, we display the charge transferred between the leads at zero bias, see Eq. (5), when slowly moving a kink along the ribbon (*adiabatic kink transition*). In the energy window considered, the ribbon dispersion relation consists of two subbands with opposite group velocities, $E_{\pm}^{(1)} = \pm \hbar v_{\text{F}} k_y$, see Fig. 1 (c). Therefore, the total charge available for transfer at the ribbon section of $L_{\text{eff}} = L - W_{\text{infty}}$ length can be estimated (up to a sign) as

$$\frac{Q_{\text{tot}}}{e} \approx \frac{|\mu_0|}{\hbar v_{\text{F}}} \frac{L_{\text{eff}}}{\pi} = 35.3 \frac{|\mu_0|}{t_0}, \qquad (6)$$

where $v_{\text{F}} = \sqrt{3}\,t_0\,a/(2\hbar) \approx 10^6\,\text{m/s}$ is the Fermi velocity in graphene and

we put $L - W_{\mathrm{infty}} = 55.5\sqrt{3}\,a$. For the strongest deformation $(H = 2\,a)$, the kink almost perfectly blocks the current flow, and the charge transferred is close to the approximation given by Eq. (6); see Fig. 3.
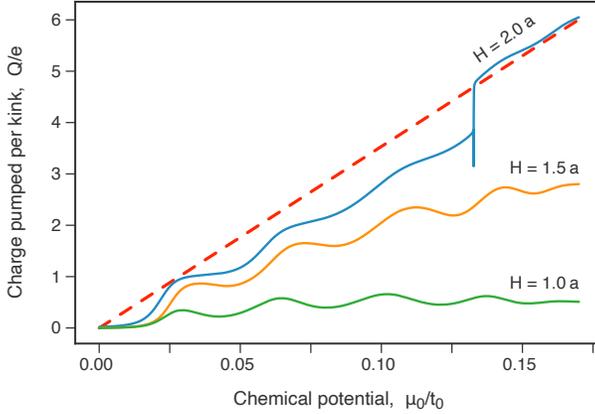

Fig. 3. Charge transferred upon adiabatic kink transition calculated from Eq. (5), for varying buckling amplitude $H/a = 1, 2$ (specified for each line in the plot), displayed as a function of the chemical potential. Dashed line shows the approximation given by Eq. (6). Remaining parameters are the same as in Fig. 2.

4. Conclusion

We have investigated, by means of computer simulations of electron transport, the operation of adiabatic quantum pump built within a topological defect moving in buckled graphene nanoribbon. We find that the pump effectiveness is close to the maximal (corresponding to a kink perfectly blocking the current flow) for moderate bucklings, with relative bond distortions not exceeding 8%. As topological defects generally move with negligible energy dissipation, we hope our discussion will be a starting point to design new graphene-based energy conversion devices.

REFERENCES

[1] Yu.V. Nazarov, Ya.M. Blanter, «Quantum Transport: Introduction to Nanoscience», *Cambridge University Press*, Cambridge 2009, Chapter 1.

[2] E. Prada, P. San-Jose, H. Schomerus, *Solid State Commun.* **151**, 1065 (2011).

[3] M. Wakker, M. Blaauboer, *Phys. Rev. B* **82**, 205432 (2010).

[4] P. San-Jose, E. Prada, H. Schomerus, S. Kohler, *Appl. Phys. Lett.* **101**, 153506 (2012).

[5] Y. Jiang *et al.*, *Phys. Rev. Lett.* **110**, 046601 (2013).

[6] E. Grichuk, E. Manykin, *Eur. Phys. J. B* **86**, 210 (2013).

[7] B. Abdollahipour, E. Moomivand, *Physica E* **86**, 204 (2017).

[8] M. Fujimoto, H. Koschke, M. Koshino, *Phys. Rev. B* **101**, 041112 (2020).

[9] R.D. Yamaletdinov, V.A. Slipko, Y.V. Pershin, *Phys. Rev. B* **96**, 094306 (2017).

[10] R.D. Yamaletdinov, T. Romańczukiewicz, Y.V. Pershin, *Carbon* **141**, 253 (2019).

[11] K. Harigaya, *Prog. Theor. Phys. Suppl.* **113**, 229 (1993).

[12] J. Ma, S. Guan, C.-H. Lai, *Phys. Rev. B* **74**, 205401 (2006).

[13] G. Dresselhaus, M.S. Dresselhaus, R. Saito, «Physical Properties of Carbon Nanotubes», *World Scientific*, Singapore 1998, Chapter 11.

[14] O. Gröning *et al.*, *Nature* **560**, 209 (2018).

[15] C.W. Groth, M. Wimmer, A.R. Akhmerov, X. Waintal, *New J. Phys.* **16**, 063065 (2014); see also: `https://kwant-project.org`